2018 20th International Symposium on High-Current Electronics (ISHCE 2018)

Tomsk, Russia
16 – 22 September 2018

IEEE Catalog Number: CFP18Q47-POD
ISBN: 978-1-5386-6892-4

***** This is a print representation of what appears in the IEEE Digital Library. Some format issues inherent in the e-media version may also appear in this print version.***

IEEE Catalog Number:	CFP18Q47-POD
ISBN (Print-On-Demand):	978-1-5386-6892-4
ISBN (Online):	978-1-5386-6891-7

Additional Copies of This Publication Are Available From:

Curran Associates, Inc
57 Morehouse Lane
Red Hook, NY 12571 USA
Phone: (845) 758-0400
Fax: (845) 758-2633
E-mail: curran@proceedings.com
Web: www.proceedings.com

Table of Contents

A High-Power Source of Ultrawideband Radiation with Reflector Antenna

Evgeny Balzovsky
Laboratory of Microwave Electronics
IHCE SB RAS
Tomsk, Russia
tduty5@mail.ru

Yury Buyanov
Laboratory of Microwave Electronics
IHCE SB RAS
Tomsk, Russia
yurbuy@yandex.ru

Vladimir Gubanov
Physical Electronics Department
IHCE SB RAS
Tomsk, Russia
gubanovvp@gmail.com

Anatoly Efremov
Pulsed Power Department
IHCE SB RAS
Tomsk, Russia
efremov@oit.hcei.tsc.ru

Vladimir Koshelev
Laboratory of Microwave Electronics
IHCE SB RAS
Tomsk, Russia
koshelev@lhfe.hcei.tsc.ru

Eduard Nekrasov
Laboratory of Microwave Electronics
IHCE SB RAS
Tomsk, Russia
a001sd@gmail.com

Alexey Stepchenko
Physical Electronics Department
IHCE SB RAS
Tomsk, Russia
lexa_stp@msn.com

***Abstract*—Characteristics of a source of linearly-polarized ultrawideband (UWB) pulse radiation based on the irradiation of a offset-parabolic reflector by a compact UWB combined antenna was investigated in the paper. The feed antenna was excited by a bipolar voltage pulse of the amplitude up 100 kV and duration of 1 ns at the pulse repetition rate of 200 Hz, The developed source is designed to use in radar with high spatial resolution and to test radio-electronic systems.**

***Keywords*—ulrawideband pulse, reflector antenna, offset reflector, high-power source, bipolar pulse**

I. Introduction

Compact UWB radiation sources are necessary to test the immunity of electronic devices to high-power pulsed electromagnetic influence. The sources create high strength of the pulsed electromagnetic field at a short distance from the antenna system. The installations designed for remote disruption of operation of electronic control systems of a car engine [1], as well as for provocation of failures in the control and navigation systems of dron aircrafts are known. Equally important is the task of protecting control and communication circuits from such impacts.

Communication and control protocols usually use frequencies ranging from 0.4 GHz to 2.5 GHz, which corresponds to the spectrum of 1-ns bipolar voltage pulses exciting the antenna. The central frequency in the spectrum of such pulses, near which the maximum energy is concentrated, is close to 1 GHz. An estimation of the peak field strength sufficient to stop the car is given in [2] and near the object it is 50 kV/m. For practical use, distances to the object exceeding 10 m are of interest. The characteristic of the source, such as the product of a peak electrical field strength E_p by a distance r to the source, should have a value no less than rE_p = 500 kV.

It is of interest to develop the pulse sources of nanosecond duration based on a parabolic reflector. There are sources having a dipole irradiator in the focus of a circular reflector [3], or a TEM horn feeder in the aperture of an offset reflector. It is promising to use a combined antenna [4] as a feed one due to its small electrical dimensions and a pattern close to the cardioid one.

To form high-voltage bipolar pulses, it is preferable to use the SINUS-160 gas discharge generator [5]. It was developed at the IHCE SB RAS and proved reliable operation in the composition of various experimental installations. However, to increase the efficiency of the functional exposure of the UWB source being developed on the objects under study, it is necessary to increase the pulse repetition rate f_p of radiation up to 200 Hz.

II. Antenna System

Antenna system consists of a parabolic reflector and a feed antenna in the form of a combined one. To prevent shading of the parabolic reflector by the feed antenna and high-voltage feeder system, it is preferable to use an offset reflector, that is, a part of the paraboloid. The model of the reflector formed by the rotation of the parabola around the x axis is shown in Fig. 1. The offset reflector is a set of points formed by the intersection of a paraboloid and a circular cylinder. The frequency range of 0.4-2 GHz, occupied by the spectrum of exciting bipolar pulses of duration 1 ns, was taken into account when choosing the size of the reflector. At the lower frequency of the spectrum, the size of the reflector should be equal at least to two wavelengths. The height and the width of the reflector manufactured by industry are chosen to be equal to 1.6 m and 1.4 m, respectively. At a lower frequency of the spectrum, the electrical dimensions are 2.1 and 1.9 of the wavelengths, and at a central frequency of 1 GHz they are 5.3 and 4.7 of the wavelengths, respectively. The focal length of

978-1-5386-6891-7/18/$31.00 ©2018 IEEE

the selected reflector is 70 cm. To create the maximum of the electric field at a distance of 5 m from the antenna, it is necessary to move the feed antenna out of focal point. A combined antenna, which is a set of electric and magnetic type radiators fed by the pulses with necessary time delays and combined by a common coaxial input, is used as a feed antenna. Such antenna was previously developed and optimized [6].

A. Simulations of Antenna and Reflector

To determine the directional-response patterns of the antenna with different position of the feed antenna relative to the point of focus, numerical simulation was carried out in the 4NEC2 software [7], which is based on the method of moments for wire structures. The geometry of the task is shown in Fig. 1. The reflector and the feed antenna are divided into cells formed by the intersection of thin wires. The software used has a limit of 11,000 wire fragments. This limit determines the size of the cells. Calculation of the task on a personal computer does not exceed two minutes at each frequency point. The results of calculating the patterns of the reflector antenna, when the feed antenna is in the focus of the reflector, correspond to the expected ones and are shown in Fig. 2. In the *H*-plane, the antenna pattern is symmetrical, as well as the symmetrical pattern of the combined antenna. In the *E*-plane, the symmetry is not observed. In the direction of the main maximum, the antenna radiation has a linear polarization.

B. Measurement of Characteristics

The results of measuring the coefficient of reflection from the feed antenna $|S_{11}|$ are shown in Fig. 3. The measurements

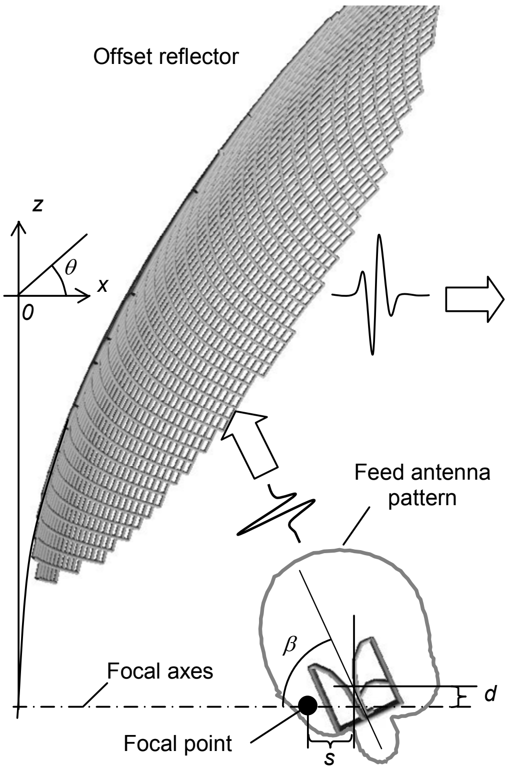

Fig. 1. Geometry of the task.

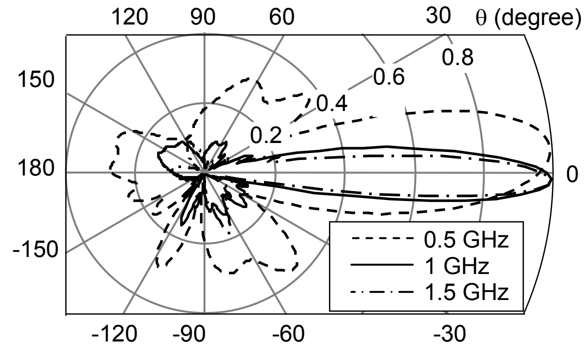

Fig. 2. Calculated patterns of the reflector antenna in the *E*-plane.

were carried out using the Agilent N5227A vector network analyzer. By the level $|S_{11}| < -10$ dB, the passband of the feed antenna is equal to 0.38-2.4 GHz. The same results are given for calculation at several frequency points.

The position of the feed antenna relative to the reflector is determined, at which the peak field strength has a maximum value at a distance $r = 5$ m at the height corresponding to the center of the reflector. The position at which the maximum of the pattern of the combined antenna is directed to the geometric center of the reflector is the optimal, and the feed antenna is moved from the focal point by 8 cm from the reflector. The measured angular distribution of the E_p field in the *E*- and *H*-planes at this position of the feed antenna is presented in Fig. 4. The range of angles at which E_p decreases by no more than 3 dB is ±5 degrees in both planes. We see that at the $r = 5$ m the area of maximum electrical field strength has a diameter of about 90 cm.

III. Design of the Source of Bipolar Voltage Pulses

The source of high-power pulsed radiation consists of three main devices. They are the following: a generator of high-voltage monopolar pulses, a bipolar pulse former, and an antenna system. The physical configurations of the generator and the pulse former are shown in Fig. 5. These devices are installed outside the shielded anechoic chamber. The generator output through the window in the anechoic chamber is

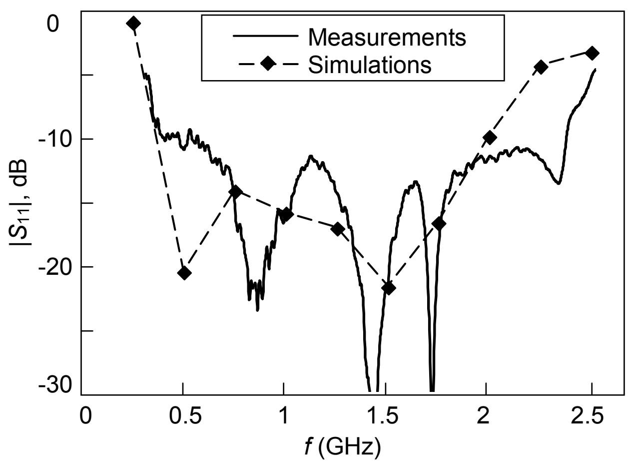

Fig. 3. The reflection coefficient from the input of the feed antenna.

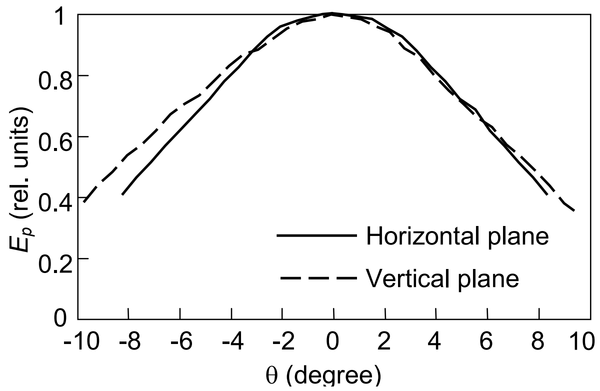

Fig. 4. Angular distribution of the peak field strength on the radiation axis at a 5 m distance from the antenna.

connected to the antenna system shown in Fig. 6. The feed antenna and the reflector are fixed on the turntable. The axis of rotation in the horizontal plane passes through the center of the feed antenna. A half-rigid coaxial cable filled with SF_6 gas is used to connect the feed antenna to the generator output. Below are descriptions of the above-mentioned devices.

A. A High-Voltage Generator of Monopolar Voltage Pulses

The SINUS-160-40 generator is used as a generator of high-voltage pulses. It was designed to generate high-power voltage pulses of about 5 ns duration and voltage on the load of up to 500 kV with f_p of up to 100 Hz [5]. To enhance the exposure of the UWB source being developed on the studied objects, the generator was modified and f_p was increased to 200 Hz.

The pulse repetition frequency is limited by factors related to the properties of a sharpening discharge switch. A region of heated gas with lower density is formed in the interelectrode gap of the switch during the operation of generator. The gas has no time to cool down between the breakdowns. A system for blow-down and change of the gaseous medium in the switch was modified to increase f_p. It was revealed that for increasing f_p up to 200 Hz, while maintaining the stored energy in the forming line, it is necessary to double the power of the supply source up to 3 kW. The capacity of the system for blowing-down the gas in the discharge gap was increased approximately two-fold. The cooling water flow in the heat exchanger and the thyristor key radiator of the primary storage were increased as well.

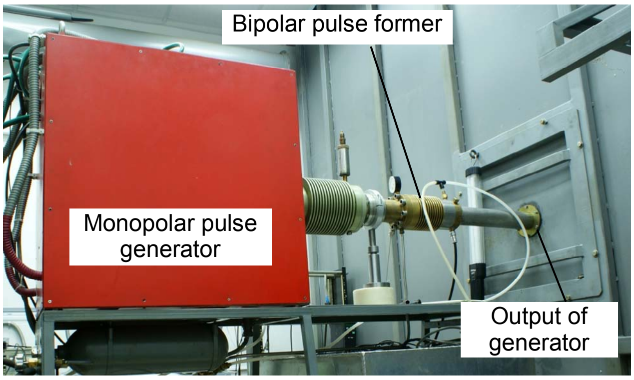

Fig. 5. Physical configuration of the source of bipolar voltage pulses.

The sharpening discharge switch has been modernized. The previously used spherical electrodes of the sharpening switch were replaced by the electrodes having a cone-shaped profile with a rounded apex. The tests revealed that stabilization of the breakdown voltage in the gaseous medium of the discharge switch requires a certain amount of air (oxygen). A special procedure for filling the discharge switch with nitrogen has been developed. First, the switch is filled with nitrogen to a pressure of about 4-5 kg/cm^2, and then the gas is released. After that, the switch is again filled with nitrogen to an operating pressure of 12-13 kg/cm^2. After switching on the generator and a series of approximately 10^5 pulses, the breakdown voltage of the switch stabilizes. The measures listed above allowed achieving the generator operation at $f_p = 200$ Hz with an instability of the breakdown voltage of the order of 1% at the output voltage of 340 kV.

B. A Former of 1 ns Bipolar Voltage Pulses

The former of high-power bipolar voltage pulses of duration 1 ns is described in detail in [5]. It is made according to the scheme with an open-circuited line and consists of decoupling inductance, four coaxial lines, a sharpening switch, and a cut-off switch. The former provides the possibility to adjust smoothly the amplitude of the output bipolar voltage pulse in the range from 100 to 200 kV by changing the nitrogen pressure in the limits of 30 to 80 kg/cm^2. The output transmission line is filled with SF_6 gas under the pressure of 5 kg/cm^2. The output bipolar voltage pulse was recorded by a divider on the coupled lines using a TDS 6604 oscilloscope with a bandwidth of 6 GHz. The waveform of the voltage pulse is shown in Fig. 7 at the start of operation and after 10 minutes of continuous work of the generator at $f_p = 200$ Hz. The decrease in the value of U_g with operating time is caused by the

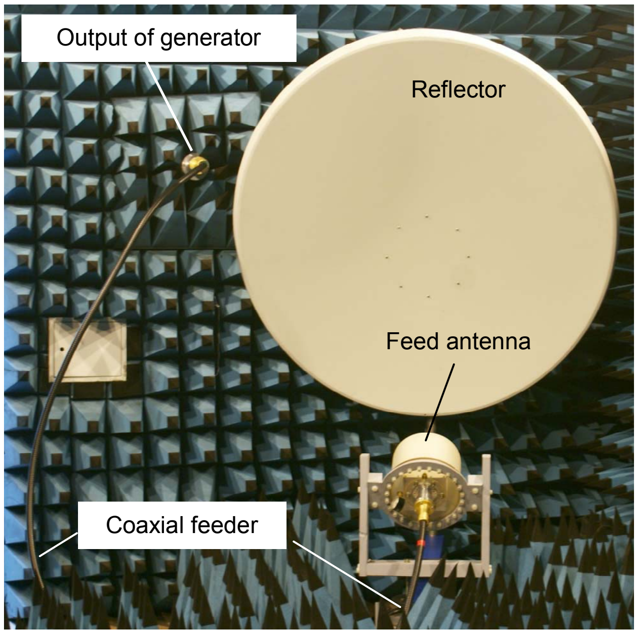

Fig. 6. Physical configuration of the antenna system installed in the anechoic chamber.

erosion of the switch electrodes in the bipolar pulse former. The value U_g can be rapidly increased to the initial one by increasing slightly the nitrogen pressure in the switch. The pulse duration at a level of 0.1 from the amplitude value is 1 ns. The root-mean-square deviation of the voltage amplitude at the output of the bipolar pulse former is no higher than 5%.

C. The Feed Antenna and High-Voltage Feeder Path

The physical configuration of the feed antenna with is shown in Fig. 8. The design and characteristics are described in detail in [6]. To prevent electrical breakdown between the electrodes, the antenna is placed in a sealed polyethylene container filled with SF_6 gas at a pressure of 1.6 kg/cm^2. The antenna is connected to the high-voltage generator through a feeder path made of RK50-17-51C semi-rigid coaxial cable with a corrugated outer conductor and insulation in the form of a spiral-shaped polyethylene. The feeder path is connected to the output of the bipolar pulse generator through a conical adapter. The length of the high-voltage feeder from the generator to the feed antenna is 4 m. The feeder path is filled with SF_6 gas at a pressure of 5 kg/cm^2.

IV. Measurement Results of Characteristics of the Source of UWB Radiation Pulses

The field strength generated by the radiation source has been measured. The measurements were carried out in a shielded anechoic chamber. When measuring the waveform of UWB pulses, a TEM antenna with a ground plate of the size 120×50 cm and a height of 8 cm was used as a receiving one. The waveform of the voltage at the TEM antenna output is proportional to the waveform of the electric field strength of the incident radiation. The effective height of the TEM antenna h_e equals to a half height of the antenna aperture and has no dependence on frequency in a wide range. High-voltage attenuators with the passband of 8.5 GHz are installed at the output of the TEM antenna. The attenuated signal $U_0(t)$ was recorded by the LeCroy WaveMaster 830Zi real-time oscilloscope. The channel of the oscilloscope with the passband of 16 GHz was used. The number of digitization points per one nanosecond was equal to 40.

Since the measuring path consisting from a set of attenuators and low-voltage measuring cables is installed between the output of the TEM antenna and input of the oscilloscope, it is necessary to take into account the attenuation and the frequency dispersion of this path. Complex forward loss $K(f)$ of the measuring path was measured by means of the Agilent N5227A network analyzer in the frequency range of 0.01-6 GHz. At the frequency of 1.1 GHz, that corresponds to the maximum of the spectrum of radiated pulses, the attenuation factor of the receiving path is $a = 73.8$ dB. The waveform of the voltage pulse $U_1(t)$ at the input of the measuring path was restored by means of the equation:

$$U_1(t) = \frac{1}{2\pi}\int_{-\infty}^{\infty} V_0(f)K(f)e^{-i2\pi ft}df,$$

where $V_0(f)$ is the complex spectrum of the voltage pulse $U_0(t)$ at the output of the measuring path, i.e., at the input of the oscilloscope:

$$V_0(f) = \int_{-\infty}^{\infty} U_0(t)e^{i2\pi ft}dt.$$

When calculating the spectrum, all readings of the voltage pulse $U_0(t)$ were supposed to be equal to zero outside the time window of the duration 10 ns.

The waveform of the restored voltage $U_1(t)$ at the output of the TEM antenna at $f_p = 100$ Hz is shown in Fig. 9. The waveform of the pulse $U_2(t)$, calculated by multiplication of the voltage $U_0(t)$ by the attenuation factor of the receiving pass, according to the equation

$$U_2(t) = U_0(t)10^{\frac{a}{20}}$$

is presented in Fig. 9 as well.

Prior to the main high-power pulse, a low-amplitude pulse is observed on the waveforms. This pulse corresponds to radiation of the feed antenna directed immediately towards the receiving antenna, without reflection from the offset reflector.

The peak strength of the field E_p has been calculated at a distance $r = 5$ m from the feed antenna, taking into account the

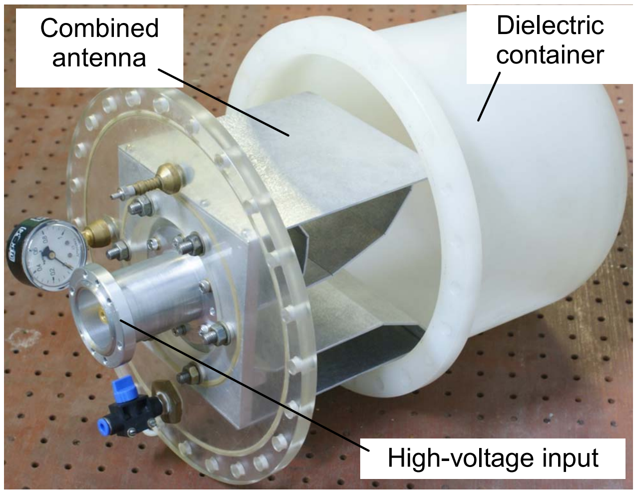

Fig. 8. The feed antenna in the dielectric case.

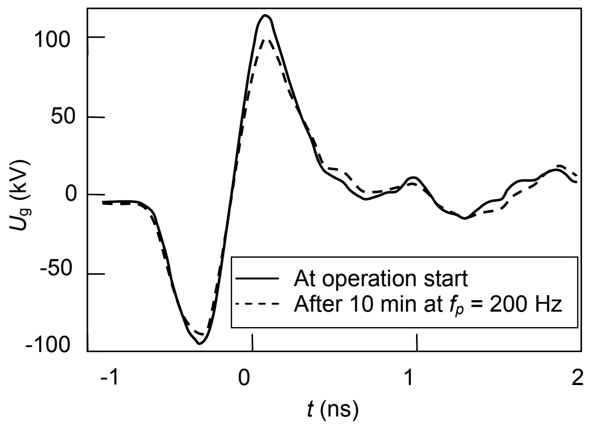

Fig. 7. Voltage pulse at the output of the bipolar pulse former.

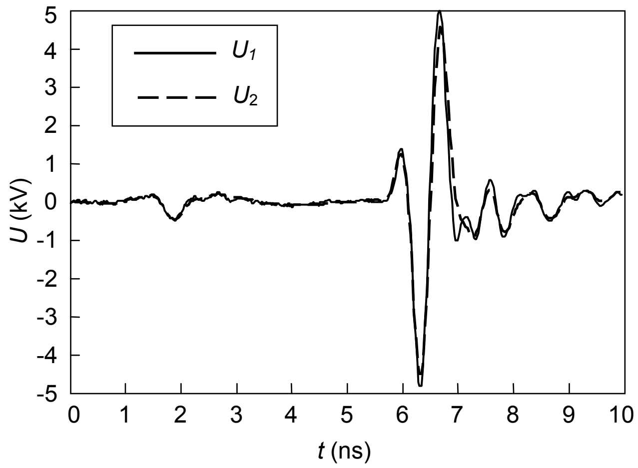

Fig. 9. Waveform of voltage pulses at the output of the receiving TEM antenna.

value of the effective length of the TEM antenna h_e = 4 cm. For the restored pulse $U_1(t)$, at f_p = 100 Hz, the value E_p is equal to 127 kV/m in the positive time lobe of the pulse and 124 kV/m in the negative one, respectively. Maximum value of rE_p equals to 630 kV. For the pulse $U_2(t)$, obtained by multiplication of $U_0(t)$ by a, E_p = 114 kV/m in the positive time lobe and 112 kV/m in the negative one, respectively. Maximum value of rE_p equals to 570 kV.

Dependence of the E_p stability on f_p and operation time of the source of radiation pulses has been studied. Dependence of E_p in the positive and negative time lobes of the pulse $U_2(t)$ is illustrated by Fig. 10a.

Increase of f_p up to 200 Hz results in the field strength decrease by no more than 20% in comparison with the initial values at a low pulse repetition rate. The average value of E_p at f_p of up to 200 Hz equals to 105 kV/m. When after the operation cycle with f_p = 200 Hz the source is switched over to f_p = 10 Hz, the E_p increases. General tendency to decrease the E_p value with time is related to the decrease of U_g. The dispersion σ of the maximum field strength E_p is shown in Fig. 10b. It was revealed that the value of σ depends weakly on the repetition rate and is within 14-16%.

V. Conclusion

The radiation characteristics of a high-power ultrawideband radiation source with a reflector antenna were studied. The geometry of the offset reflector and the position of the feed antenna were calculated. The feed antenna position relative to the reflector focus was determined to obtain the maximum field strength at a distance of 5 m from the antenna. The source of the voltage pulses was modernized to operate at a pulse repetition rate of 200 Hz. The pulse duration at the output of the high-voltage bipolar pulse former is 1 ns by the level of 0.1. The waveform of the pulsed electric field strength at a distance of 5 m from the antenna was measured. The average value of the peak field strength for a sample of $1.2 \cdot 10^5$ pulses is 105 kV/m with the voltage at the output of the bipolar pulse generator of 100 kV. The product of the peak electric field strength of the developed source by the distance exceeds 500 kV.

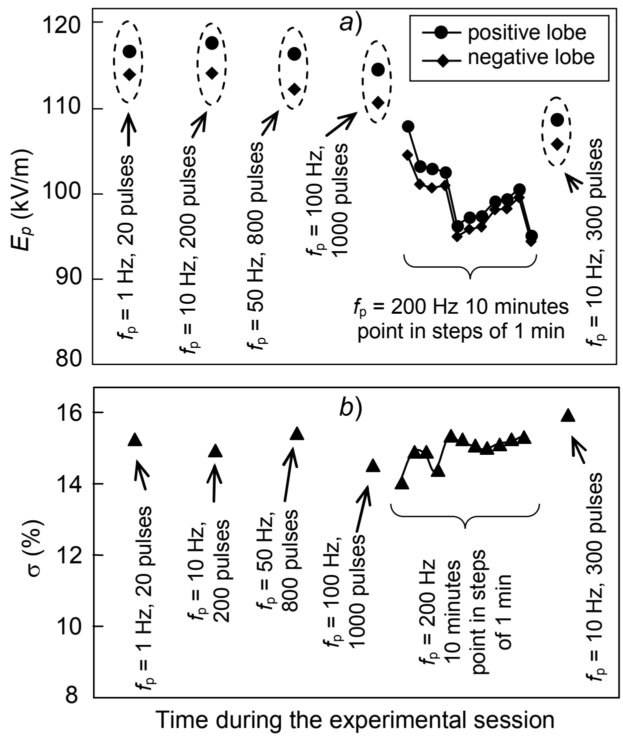

Fig. 10. The peak field strength at a 5 m distance from the source (a) and the peak field strength dispersion (b) versus f_p and operation time.

Acknowledgment

The authors are grateful to the Center for Collective Usage of the Tomsk Scientific Center of the Siberian Branch of the RAS for the provided LeCroy Wave Master 830-Zi oscilloscope and the Agilent N5227A network analyzer.

References

[1] R. Przesmycki, “Directed Energy Applications to the Destruction of Informatic Devices,” in PIERS Proceedings, Jul. 2015, pp. 292–296.

[2] K. Hong and S. Braidwood, “Stopping car engines using high power electromagnetic pulses,” in Proc. Int. Conf. Electromagn. Adv. Appl., 2010, pp. 378–381.

[3] J. Ryu, J. Lee, H. Chin, J.-H. Yeom, H.-T. Kim, H.-O. Kwon, S. H. Han, and J. S.Choi, “A high directive paraboloidal reflector antenna for high far voltage in an ultra wideband source system,” IEEE Trans. on Plasma Sci., vol. 41, pp. 2283–2290, Aug. 2013.

[4] Yu. A. Andreev, Yu. I. Buyanov, and V. I. Koshelev, “A combined antenna with extended bandwidth,” J. Comun. Technol. Electron., vol. 50, pp. 535–543, 2005.

[5] A. M. Efremov, V. I. Koshelev, B. M. Koval’chuk, V. V. Plisko, and K. N. Sukhushin, “Generation and radiation of high-power ultrawideband nanosecond pulses,” J. Comun. Technol. Electron., vol. 52, pp. 756–764, 2007.

[6] E. V. Balzovsky, Yu. I. Buyanov, V. I. Koshelev, and E. S. Nekrasov, “Ultrawideband combined antenna with improved matching,” IOP Conf. Ser.: Mater. Sci. Eng., vol. 363, p. 012002, 2018.

[7] A. Voor. (2018). NEC based antenna modeller and optimizer [Online]. Available: http://www.qsl.net/4nec2/